Journal of Materials Chemistry B

ROYAL SOCIETY OF CHEMISTRY

PAPER

View Article Online
View Journal | View Issue

Cite this: J. Mater. Chem. B, 2025, 13, 14425

Innovative hyaluronan/gellan gum/hydroxypropyl methyl cellulose membrane for prevention of adhesion in postoperative achilles tendon

Shan-Wei Yang,[abc] Mu-Ting Li,[d] Chun-Shien Wu,[e] Joseph Yang,[f] Daniel Yang[f] and Shyh-Ming Kuo*[d]

A novel anti-adhesion barrier membrane composed of FDA-approved hyaluronan (HA), gellan gum (GG), and hydroxypropyl methylcellulose (HPMC) was developed to prevent postoperative tendon adhesion in our study. Seprafilm, a commercial hydrogel barrier membrane comprising HA and carboxymethyl cellulose (CMC), is effective in abdominal surgeries to reduce postoperative adhesions between the abdominal wall and underlying tissues. However, it is fragile, difficult to handle, and degrades rapidly, limiting its barrier function. Our HA/GG/HPMC (HGH) membrane overcame these drawbacks, exhibiting superior resilience, hydrophilicity, water content, swelling ratio, and stress–strain properties compared to the HG (HA/GG) and Seprafilm membranes. The HGH membrane was highly hydrophilic and reached hydration equilibrium within 3 min, enabling it to wrap tendons snugly without sticking or tearing. It degraded more slowly (60% mass remaining after 12 days *in vitro*, *vs.* 15% for Seprafilm after 4 days), providing an extended protective presence during the tendon's healing period. In a rat Achilles tendon repair model, the HGH membrane significantly reduced peritendinous adhesions and facilitated better healing histologically. The repaired tendon breaking strength after 3 weeks was significantly higher in the HGH group (37.5 N) than in the untreated (6.5 N), HGC (16 N), or Seprafilm (15.5 N) groups. Haematoxylin and eosin staining indicated that the HGH membrane resulted in significantly less tendon–tissue adhesion and superior healing. In summary, the HGH membrane degraded more slowly, was less fragile, more resilient, and more hydrophilic, making it easier to handle during surgery and thus an effective candidate for preventing adhesions in tendon surgery.

Received 24th July 2025,
Accepted 6th October 2025

DOI: 10.1039/d5tb01703c

rsc.li/materials-b

1. Introduction

After surgery, tissue adhesions may develop because of inflammation and the growth of fibrous tissue during the healing process. Adhesions are a natural reaction of the body's tissues during wound healing. Approximately 90% of abdominal surgeries may cause adhesions of varying severity levels. Various strategies have been employed to prevent such adhesions, including the administration of drugs (*e.g.*, nonsteroidal anti-inflammatory drugs, corticosteroids, and fibrinolytic agents), the use of minimally invasive surgical techniques, and the application of physical barriers.[1–3] Moreover, adhesion prevention materials (*e.g.*, absorbent films) can help when necessary.[4]

After tendon repair surgery, the risk of adhesion between the surgical tendon and the synovial sheath is relatively high. Postsurgical adhesion in the tendon interferes with the normal gliding function of the tendon and nerves and thus causes pain and restricts motion. Several studies have proposed hydrogel barriers for preventing the adhesion of a repaired tendon to surrounding tissues; nevertheless, such barriers often involve reactive agents (including plant extracts or chemicals such as gallic acid, tannic acid, dopamine, and polydopamine) that may complicate commercial use.[5–8] For improved simplicity and commercial viability, using pure and Food and Drug Administration (FDA)-approved materials may be a more favorable alternative.

Certain commercial medical products have antiadhesive properties. For example, Seprafilm is a bioresorbable adhesion barrier (Genzyme, Cambridge, MA, USA) composed of hyaluronan (HA) and carboxymethyl cellulose (CMC). Seprafilm is

[a] Department of Orthopedics, Kaohsiung Veterans General Hospital, Kaohsiung City 813414, Taiwan
[b] School of Nursing, Fooyin University, Kaohsiung City 831301, Taiwan
[c] Department of Leisure and Sports Management, Cheng Shiu University, Kaohsiung City 833301, Taiwan
[d] Department of Biomedical Engineering, I-Shou University, Kaohsiung City, Taiwan. E-mail: smkuo@isu.edu.tw
[e] Center of General Education, I-Shou University, Kaohsiung City, Taiwan
[f] Cambridge International Programme, St. Dominic Catholic High School, Kaohsiung City 802306, Taiwan

indicated for use in patients undergoing abdominal or pelvic laparotomy as an adjunct for reducing the incidence, extent, and severity of postoperative adhesions; it helps prevent adhesions between the abdominal wall and underlying viscera, such as the omentum, small bowel, bladder, and stomach, as well as between the uterus and adjacent structures, including the fallopian tubes, ovaries, large bowel, and bladder. The barrier degrades within 7 days at the site of its application.[9] Although Seprafilm is not commonly used in routine tendon surgery and the fast degradation is a concern, it has been tested or considered off-label in contexts outside abdominal surgery, including tendon repair research, due to the lack of tendon-specific commercial barriers. Some studies have also explored its preventive adhesion effect in tendon injury animal models.[10–13] Kohanzadeh *et al.* also reported that Seprafilm was a safe and helpful tool for decreasing or even preventing adhesion formation in the wrist and hand surgery of their patients.[14] Although Seprafilm has been proven safe and effective, it has several drawbacks; for example, it is expensive, can degrade too rapidly, is fragile, is relatively difficult to shape, and is difficult to wrap around non-flat surgical sites such as tendons. These disadvantages adversely affect postoperative patient management and interventions and lead to increased healthcare costs. Additionally, studies have reported challenges in handling Seprafilm. For example, Seprafilm is inherently fragile in its dry state and somewhat stiff and brittle. Once moistened, it becomes extremely sticky, which hampers its handling during surgery. Seprafilm also poses some practical concerns because it may interfere with tissue healing. Wrapping an anastomosis with Seprafilm has been reported to significantly increase the risks of anastomotic leaks and related complications, such as fistulas and abscesses.[15] In one study, Seprafilm interfered with intestinal healing when placed too close to suture lines. Therefore, Seprafilm should not be applied near anastomotic sites, as it may impair healing or cause fluid buildup around the new connection, which can lead to inflammation. Furthermore, Seprafilm is a flat sheet designed for use on flat surfaces inside the abdominal wall; consequently, efficiently applying it to curved or small tissues such as tendons is challenging. Accordingly, addressing the aforementioned drawbacks of Seprafilm is essential to enhance its effectiveness and support broader commercial applications.

Hydroxypropyl methylcellulose (HPMC) is a cellulose ether formed by the substitution of the hydroxyl groups of cellulose with methyl and hydroxypropyl groups. The substitution of free hydroxyl groups of glucose with hydroxypropyl groups improves the cellulose backbone in terms of viscosity, solubility, gelation, and film-forming behavior. Methyl groups contribute to the stability and hydrophobicity of HPMC. HPMC is commonly used as a high-performance film-forming material because of its favorable miscibility with a wide range of organic and inorganic materials.[16–18] Habibullah, SK *et al.* utilized carboxymethylated gum combined with HPMC-nanocellulose to fabricate moxifloxacin-containing composite film to improve the ocular inflammation and antimicrobial activities. They demonstrated that the presence of polar hydroxypropyl groups in HPMC improved the mechanical properties due to increased intermolecular interactions with the hydroxy groups of the carboxymethylated gum in the film. Also, HPMC demonstrated a longer residence time and stability in the existence of light, temperature, and sensible levels of humidity, making it a suitable polymer for slow release of moxifloxacin to improve the management of ocular inflammation.[19] Anandalakshmi used HPMC as a gelling agent to prepare hydrogel films for wound healing delivery. These HPMC films could release the tetracycline in a sustained manner and show significant antibacterial activity after three days of release at 37 °C in PBS (pH 7.4).[20] Therefore, HPMC is widely used as an excipient in pharmaceutical formulations to help control the release of drugs and the disintegration of tablets. CMC, another cellulose derivative, is produced by placing carboxymethyl groups in the cellulose backbone. CMC is mainly used in the food industry as a thickener, stabilizer, and binder; it is also used in pharmaceutical tablet formulations as a binder.[21] Although HPMC and CMC have the exact cellulose origins, HPMC is clearly more advantageous. Specifically, HPMC exhibits excellent biocompatibility and strong resistance to enzyme degradation, making it a preferred choice for use as a sustained-release material, tablet adhesive, and thickener in ophthalmic eye drops and pharmaceutical preparations.[19] Moreover, HPMC is not easily degraded by human enzymes and can ensure the sustained release of drugs. By contrast, CMC has weaker enzyme resistance and is more easily degraded in the body, which affects its stability in pharmaceutical preparations. In summary, HPMC is superior to CMC in terms of temperature resistance, pH stability, water retention, and resistance to enzyme degradation. Despite this, most commercial antiadhesive membrane products are fabricated using CMC rather than HPMC.

Gellan gum (GG), a linear anionic polysaccharide, is employed as a stabilizer, thickening agent, and gelling agent in various food applications.[22,23] After GG was approved by the FDA in 1992 to be used as a food additive, the interest in GG for biomedical and pharmaceutical fields has vastly increased due to its biocompatibility and biodegradability. Furthermore, GG-based materials produced by the casting solvent method are primarily used in wound healing and bone tissue engineering due to their low cost, availability, and excellent film-forming properties.[24] Kim and colleagues combined demineralized bone powder with GG using the casting solvent method to fabricate scaffolds for bone regeneration. They demonstrated this scaffold under the composition of 1% demineralized bone powder/GG, which displayed proper mechanical properties, porosity, and degradation, yielding superior osteochondral regeneration in rats.[25] Chen and coworkers developed an *in situ* gelling system composed of breviscapine incorporated into GG, which underwent a sol–gel transition and significantly enhanced drug residence time, thereby improving drug bioavailability.[26] Overall, GG exhibits exceptional gelation properties, forming a highly stable hydrogel network that can be utilized in various fields.

Considering the limitations of existing commercial membranes (even those used off-label) and the favorable properties of HPMC and GG, this study aimed to fabricate membranes for

preventing adhesion between a repaired tendon and surrounding tissues. To ensure the safety of the materials used and ease of commercialization, only FDA-approved materials were employed in the fabrication; no additional extracts or chemical agents were included. The membranes were prepared using a solvent casting method and various formulations of HA, GG, HPMC, and CMC. The membranes' basic properties, including hydrophilicity, water content (WC), swelling ratio (SR), mechanical strength, and degradation, were examined to assess their handling and performance during surgical procedures. Furthermore, we utilized a rat model to assess the ability of these membranes to prevent adhesion of the repaired Achilles tendon. No commercial barrier product exists for tendon-specific adhesion prevention, so we are using Seprafilm to compare our membrane to the closest available solution. We aimed to demonstrate that our HA/GG/HPMC membrane could potentially offer advantages over what a surgeon might otherwise resort to (even if off-label) for tendon surgery.

2. Materials and methods

2.1. Materials

HPMC (M.W. 22 kDa), CMC (M.W. 90 kDa), GG (M.W. 1000 kDa), HA (M.W. 1200 kDa), and dimethyl sulfoxide (DMSO) were purchased from Sigma (St. Louis, MO, USA). Seprafilm was purchased from Baxter International Inc. (USA). We obtained 3-(4,5-dimethylthiazol-2-yl)-2,5-diphenyltetrazolium bromide (MTT), Dulbecco's modified Eagle medium (DMEM), fetal bovine serum, streptomycin, and penicillin from Gibco (Waltham, MA, USA). All chemicals used in this study were of reagent grade. Animal experiments conducted in this study were approved by the Institutional Animal Care and Use Committee of I-Shou University, Kaohsiung, Taiwan (IACUC-ISU-112–054, approval date: 19 Jan 2024).

2.2. Fabrication of hydrogel membranes

Three membranes with distinct weight ratios of HA, GG, HPMC, and CMC were prepared, and their basic properties were evaluated (Table 1). HA (53.4 mg) and GG (163.3 mg) were dissolved in 2 and 8 mL of 70 °C deionized water, respectively, and these two solutions were then mixed together. Subsequently, 1 mL of HPMC (2 wt%) or 1 mL of CMC (2 wt%) was added to the mixture, which was stirred to generate a transparent solution. Each solution was next then poured into its own glass dish and evaporated in an oven at 40 °C to yield two dry membranes. These dry membranes were crosslinked using 15 mM 1-ethyl-3(3-dimethylaminopropyl)-carbodiimide/(*N*-hydroxysuccinimide) (EDC/NHS) solution; the crosslinking was performed for 6 h at room temperature. The crosslinked membranes (denoted HG, HGH, and HGC, as listed in Table 1) were washed three times with 95% ethanol and then dried at room temperature.

Table 1 Composition of three fabricated membranes and weight ratios of constituents

Formulation content	GG (2 wt%)	HA (2.6 wt%)	CMC (2 wt%)	HPMC (2 wt%)
HG	8 mL	2 mL	—	—
HGC	8 mL	2 mL	1 mL	—
HGH	8 mL	2 mL	—	1 mL
Seprafilm	—	—	—	—

2.3. Characterization of hydrogel membranes

2.3.1. Fourier-transform infrared analysis. Fourier-transform infrared (FTIR, Agilent Cary 630, CAL, USA) spectroscopy was performed to determine the characteristic spectral peaks of the fabricated HGH and HGC membranes as well as those of the commercial Seprafilm membrane.

2.3.2. Contact angle measurement. The hydrophilicity of the fabricated membranes was characterized by measuring their water contact angles. The apparatus used for these measurements included a digital camera (Nikon Coolpix 995; Nikon, Tokyo, Japan) with a microscopic lens (CFI Plan Fluor Series Objective Lenses, Nikon) and a micropipette (Pipetman, Gilson, Villiers-le-Bel, France). Prior to the measurements for each membrane, 20 μL of deionized water was applied to hydrate it. Subsequently, 5 μL of deionized water was dropped onto the membrane, and after 3 s (to ensure the water had stabilized), a cross-sectional image of the water droplet on the membrane was captured. The contact angle was the angle at the junction between the water droplet, the membrane, and the air. All measurements were performed using a standard goniometer, which includes a digital camera (Nikon, Tokyo, Japan). Six independent measurements were performed for each membrane.

2.3.3. Water content, swelling ratio, and degradation. The water content (WC) and swelling ratio (SR) of the fabricated membranes were determined by placing the membranes in phosphate-buffered saline (PBS; pH 7.4) at room temperature. The membranes were immersed for 3 and 60 min. Once the membranes had equilibrated with the PBS, they were blotted using filter paper to remove the water molecules adhering to their surface. The WC and SR of the membranes were calculated as follows:

$$\mathrm{WC}\ (\%) = (W_\mathrm{w} - W_\mathrm{d})/W_\mathrm{d} \times 100\%$$

$$\mathrm{SR}\ (\%) = (W_\mathrm{w} - W_\mathrm{d})/W_\mathrm{w} \times 100\%$$

where W_w and W_d are the weights of the wet and dry membrane, respectively. All measurement procedures were conducted in triplicate.

The degradation of the membranes was tested by incubating them in 10 mL of PBS (pH 7.4) in a vial and placing the vial on a shaker set at 40 rpm and 37 °C. At predetermined times (every day up to 12 days), each membrane was removed from the incubation medium, washed with distilled water, dried, and weighed, after which 10 mL of fresh PBS was added to the vial and the degradation test was continued. Degradation profiles were obtained as the cumulative weight loss of the membranes.

2.3.4. Mechanical strength measurement. The fabricated membranes swelled considerably in solution and could not be mounted firmly onto a load cell, which is typically used in

mechanical strength measurements. Therefore, we conducted our mechanical strength tests with dry membranes and compared the strengths of the fabricated membranes with those of Seprafilm. Each membrane was cut into pieces measuring 1 cm × 6 cm, and its tensile strength and strain at break were measured. The mechanical parameters of the membranes were automatically calculated and recorded using a material testing system with a crosshead speed of 5 mm min^{-1}.

2.4. Cell viability assay

In accordance with the ISO 10993 guidelines on biocompatibility evaluations, extraction was performed using a material-to-extractant ratio of 0.2 g mL^{-1}. Membrane materials subjected to biocompatibility evaluations must be thinner than 0.5 mm. Accordingly, extraction was conducted at a surface-area-to-volume ratio of 6 cm^2 mL^{-1} in serum-free cell culture medium. First, the membranes were incubated in an incubator at 37 °C and under 5% CO_2 for 24 h. After this incubation, the extracts were centrifuged at 1300 rpm for 5 min. The supernatant was collected and filtered through a 0.1-μm membrane to obtain the final extract solution. The MTT assay was used to evaluate cell viability. Tenocytes (2.0×10^4 cells per well) were cultured for 24 h with the extract solutions prepared from the hydrogel membranes. Subsequently, MTT solution was added to each well at a final concentration of 0.5 mg mL^{-1}, and the cells were incubated for an additional 3 h. After the incubation period, the supernatant in each well of the 96-well plate was carefully removed, and 200 μL of dimethyl sulfoxide was added to each well to dissolve the formazan crystals completely. The optical density (OD) of each well was then measured at 450 nm by using a microplate reader (Thermo Scientific, Waltham, MA, USA). A higher absorbance value indicated higher cell viability. The mitochondrial activity of cells in each group was quantified using the following equation:

$$\text{Cell viability } (\%) = \frac{\text{Experimental value OD}_{450}}{\text{Control value OD}_{450}} \times 100\%$$

where the control value was obtained with cells cultured in a well that did not contain any extract.

2.5. *In vivo* animal study—tendon rupture and repair model

Nineteen 8-week-old male Sprague-Dawley rats (weighing 250–300 g) were anesthetized using transabdominal injections of Zoletil 50 (a 1 : 1 mixture of tiletamine and zolazepam) at a dose of 0.2 mL/200 g bodyweight. For each animal, the hind leg was shaved and then sterilized. A sharp dissection was made to expose the Achilles tendon, which was then transected at its midpoint. The transected tendon was sutured with 5-0 Prolene sutures (Ethicon, Somerville, NJ, USA). Then it was wrapped with a membrane (HGC, HGH, or Seprafilm membrane for the HGC, HGH, and Seprafilm groups, respectively). In some rats, the tendon was repaired, but a membrane was not applied (the untreated group); in others, the tendon was not ruptured (the control group). After the completion of the surgical procedure, the animals were returned to their cages and allowed to recover for 3 weeks, during which they were checked daily for signs of appetite changes, wound infections, and leg swelling. After 3 weeks, the animals were sacrificed through an overdose of isoflurane (10%), and gross evaluations were performed; moreover, histological assessments were conducted using hematoxylin and eosin (H&E) and Masson's trichrome staining to evaluate adhesion and the healing of tendons, and a tendon-breaking force test was performed on the repaired tendons. Fig. 1 illustrates the surgical process executed in the animal study and the evaluations of adhesion, inflammation, and healing of the repaired tendons.

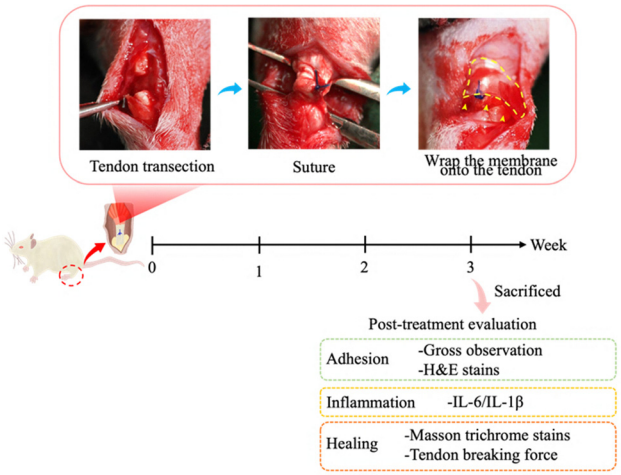

Fig. 1 Experimental design and surgical procedures of the *in vivo* animal study.

2.5.1. Macroscopic evaluation. To perform the macroscopic evaluations, three legs were randomly selected from each group (n = 3). After the animals were sacrificed, a midline incision was made in the hind leg to expose the repaired Achilles tendon. The macroscopic severity of the adhesion around the repaired tendon was evaluated using a five-grade adhesion-scoring system:[27] Grade 1, no marked adhesion; Grade 2, filmy adhesions easily separated using blunt dissection; Grade 3, ≤50% of adhesions separable using sharp dissection only; Grade 4, 51–97.5% of adhesions separable using sharp dissection; and Grade 5, >97.5% of adhesions separable using sharp dissection. All macroscopic evaluations were performed by an investigator who was blinded to the grouping.

2.5.2. Histological evaluation. Three repaired tendons in each group (the three that were not used in the gross evaluation) underwent histological examination. The heel tendon site was harvested from the tendon insertion of the calcaneal bone to parts of the gastrocnemius and soleus muscle complex. Each specimen was immersed in 10% buffered formalin for 24 h, dehydrated using an ascending graded series of ethanol solutions, and then embedded in paraffin wax. Each specimen was sectioned sagittally and stained with H&E. In the histological examination, adhesions were graded according to the proportion of the tendon surface they covered: Grade 1, no adhesions; Grade 2, mild adhesion (<33% of the tendon surface covered); Grade 3, moderate adhesion (34–66% of the tendon surface covered); and Grade 4, severe adhesion (>66% of the tendon

surface covered).[28] Tendon healing was also evaluated using Masson's trichrome stains and graded as follows: Grade 1, excellent healing (favorable tendon continuity and smooth epitenon surface); Grade 2, good healing (intratendinous collagen bundles exhibiting good repair, but epitenon interrupted by adhesions); Grade 3, fair healing (irregularly arranged and partly disrupted intratendinous collagen bundles); and Grade 4, poor healing (failed healing or overgrowth of granulation tissue).

2.6. Inflammatory interleukin-6 and interleukin-1β assay

The tissues surrounding each tendon were collected, weighed, homogenized, and centrifuged, after which the medium was collected. To detect the levels of cytokines (interleukin IL-6 and IL-1β), an enzyme-linked immunosorbent assay (ELISA) was performed using corresponding kits (Thermo Scientific, Waltham, MA, USA). The samples were processed in accordance with the kit manufacturer's instructions.

2.7. Tendon breaking force measurement

To measure the breaking strength of the repaired tendons, three tendons in each group were dissected and harvested together with the calcaneal bone and parts of the gastrocnemius muscle and soleus muscle complex. The two ends of a specimen were fixed using clamps, and the breaking force of the tendon specimen was measured at the point of tendon failure. Sandpaper and tape were inserted between the clamp and tendon sample to increase friction to prevent tendon slippage during the mechanical test (Fig. S3). Mechanical parameters were automatically calculated and recorded using an MTS (QTest/10, MN, USA) at a crosshead speed of 5 mm min^{-1}.

2.8. Statistical analysis

Data are presented as the mean ± standard deviation (SD). A one-way analysis of variance was used to compare the biomechanical results for the different repaired tendons. A two-way analysis of variance was employed to compare the WC, degradation, and mechanical strength of the membranes in the various groups. The results of the gross evaluations and histological assessments of tendon adhesion and healing were analyzed using the Wilcoxon signed-rank test. All statistical analyses were performed using SPSS (Statistical Package for Social Science; version 20.0; SPSS, Chicago, IL, USA), and $p < 0.05$ was considered significant.

3. Results and discussion

3.1 Gross observation and FTIR analyses of the membranes

This study used FDA-approved materials and crosslinking agents to fabricate antiadhesive hydrogel membranes to overcome the limitations of the available commercial products, such as Seprafilm. In brief, the aim of this study was to evaluate the effects of adding HPMC and CMC to base membranes composed of HA and GA; the study compared the membranes' basic properties, surgical usability, and antiadhesion capability in repaired rat tendons. Before HPMC or CMC inclusion was considered, we tested various GG–HA formulations and identified the formulation that resulted in a membrane with the highest mechanical strength and ease of fabrication. As shown in Fig. 2a, a GG : HA volume ratio of 8 : 2 resulted in the best mechanical strength and the least flowing and fragile membrane. By contrast, the volume ratio of 5 : 5 resulted in a membrane with softer characteristics in the flowing band.

Fig. 2b depicts the carbodiimide-mediated coupling reaction, performed using the EDC/NHS method, used to create a crosslinked, amide-bond-containing, biopolymer hydrogel network from GG, HA, and HPMC. In the covalent crosslinked hydrogel or polymeric network, GA is covalently attached to HA and/or HPMC through amide linkages (→GG–CONH–HA/HPMC). The resulting structure exhibits favorable mechanical properties and biocompatibility for biomedical applications, such as hydrogels, and may offer controlled drug delivery, be utilized for tissue scaffolding, or have wound healing applications. Optical (square area) and SEM (circular area) images of the membranes indicated that their surface topography was homogeneous (due to use of the mold-casting method). Notably, the HGH membrane seemed more resilient and flatter than the HG and HGC membranes (Fig. 2b).

Fig. S1 presents the FTIR spectra of the crosslinked biopolymer hydrogels, indicating that the network formed through characteristic functional group interactions. A broad absorption band was observed at 3400–3200 cm^{-1}, attributed to O–H and N–H stretching vibrations, indicating the presence of –OH and $–NH_2$ groups in the hydrogel matrix and suggesting that hydrogen bonding within the polymer network was extensive. Moreover, peaks were observed at approximately 2900 cm^{-1}; these were attributed to C–H stretching from aliphatic $–CH_2$ and $–CH_3$ groups, primarily originating from HPMC. A sharp absorption band was noted at 1750–1700 cm^{-1} and was assigned to the –C═O stretching vibrations of ester and –COOH groups, confirming the existence of crosslinked structures involving HA and GG. Furthermore, amide I and amide II bands were observed at approximately 1650 and 1550 cm^{-1}, respectively, confirming the formation of amide bonds, which likely resulted from crosslinking reactions between –COOH and $–NH_2$ groups. Additional peaks were identified at 1250–1000 cm^{-1} and were attributed to C–O–C stretching and C–OH bending vibrations, which could be attributed to the polysaccharide backbones of GG and HPMC, as well as possible ether linkages. Furthermore, bands were observed at approximately 890–840 cm^{-1}, which are characteristic of β-glycosidic linkages, supporting the polysaccharide structure of the hydrogel components. Comparative analysis revealed differences between the spectra of the different membranes, particularly in terms of the intensity of peaks associated with –C═O and ether groups. This finding indicates variations in crosslinking density and composition among the different membranes.[14,29] Overall, the FTIR analysis confirmed that GG, HA, and HPMC had been successfully integrated into a crosslinked hydrogel network (GG–CONH–HA/HPMC) through both physical

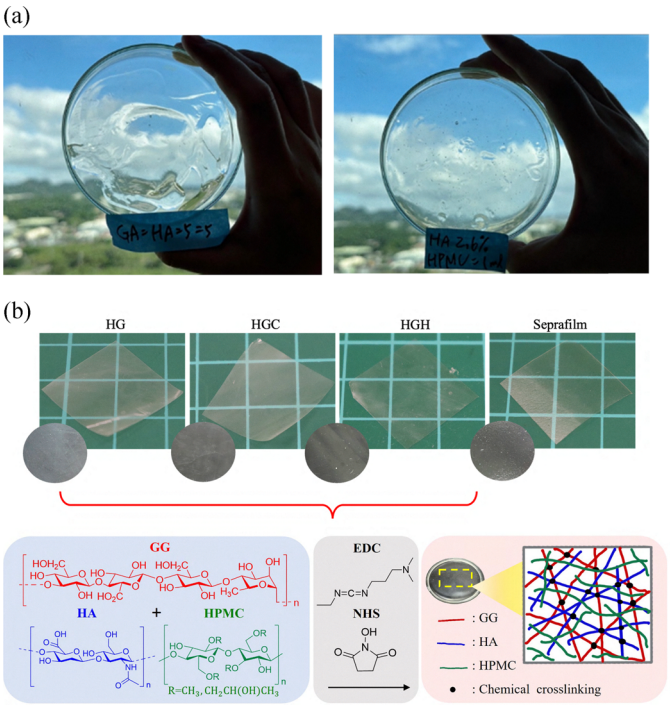

Fig. 2 (a) Images of membranes prior to the addition of CMC or HPMC solution. Left: GG : HA ratio = 5 : 5. Right: GG : HA ratio = 8 : 2. (b) Gross observations of hydrogel membranes, and a schematic of the fabrication of the HGH membrane when using EDC/NHS as the crosslinking agent.

(hydrogen bonding) and chemical (amide and ester) interactions. Overall, the characteristic peaks in the spectra of the HGC, HGH and Seprafilm membranes indicated that these membranes had similar structures.

3.2 Characterization of HGC, HGH, and Seprafilm membranes

Contact angle measurements provide valuable insights into the wettability of a surface, with smaller angles indicating better wetting (hydrophilicity) and larger angles indicating poorer wetting (hydrophobicity). Contact angles are usually measured using the sessile drop method. As illustrated in Fig. 3a, the HGC and HGH membranes had smaller contact angles than the HG and Seprafilm membranes did, indicating that the addition of CMC and HPMC components resulted in a more hydrophilic surface. The range of contact angles for the Seprafilm membrane was similar to that for the HG membrane (Table 2). A hydrogel membrane being used in a surgical procedure for preventing adhesion should reach hydration equilibrium within a few minutes. As displayed in Fig. 3b, the WC of the membranes increased by approximately 80–90% within 3 min of immersion in distilled water and was not considerably different after a longer 60-min immersion. This signifies that the membranes reached hydration equilibrium as required. Similarly, the SR stabilized within 3 min (Fig. 3c). The WC and SR of the HGH membrane were significantly higher than those of the HG, HGC, and Seprafilm membranes.

To be used in clinical applications, antiadhesion membranes must also degrade within a suitable period to maintain their barrier function. In clinical practice, such membranes are used as antiadhesive barriers after abdominopelvic surgery and must retain their barrier function for approximately 1 week. However, tendons heal more slowly than abdominal sites for weeks, and a barrier membrane for tendons must thus last a more extended period. Tendon healing begins with an acute inflammatory stage immediately (roughly the first week post-injury), followed by fibroblastic/proliferative stage (1–3 weeks post-injury), and remodeling/maturation stage (3–6 weeks post-injury). Considering tendon adhesion, the fibroblastic/proliferative stage is the key period when adhesions begin to form, where fibrous tissue bridges the healing ligament with the surrounding capsule, synovium, or fat pad.

As presented in Fig. 3d, the HG, HGC, and HGH membranes degraded slowly, losing 40–70% of their initial mass after an 11-day shaking test. However, the Seprafilm membrane began to degrade on the first day and had lost approximately 85% of its initial mass (only 15% mass remaining) after a 4-day shaking test. Using HA, GA, CMC, and HPMC to fabricate hydrogel membranes in this study resulted in a product that degraded less quickly than Seprafilm did; the degradation of the HGH membrane was especially slow, and it presented 60% mass remaining after 12 days. The HGH membrane with slower degradation could remain functional for a longer period, potentially better matching the fibroblastic/proliferative stage (1–3 weeks post-injury) than Seprafilm. Our results suggest that the membranes fabricated in this study can meet the degradation requirements for antiadhesive membranes used on slow-healing tendon tissues. Although the 12-day degradation test was not long enough to cover the full tendon healing stage, and it was our study limitation, our 12-day *in vitro* test presented a

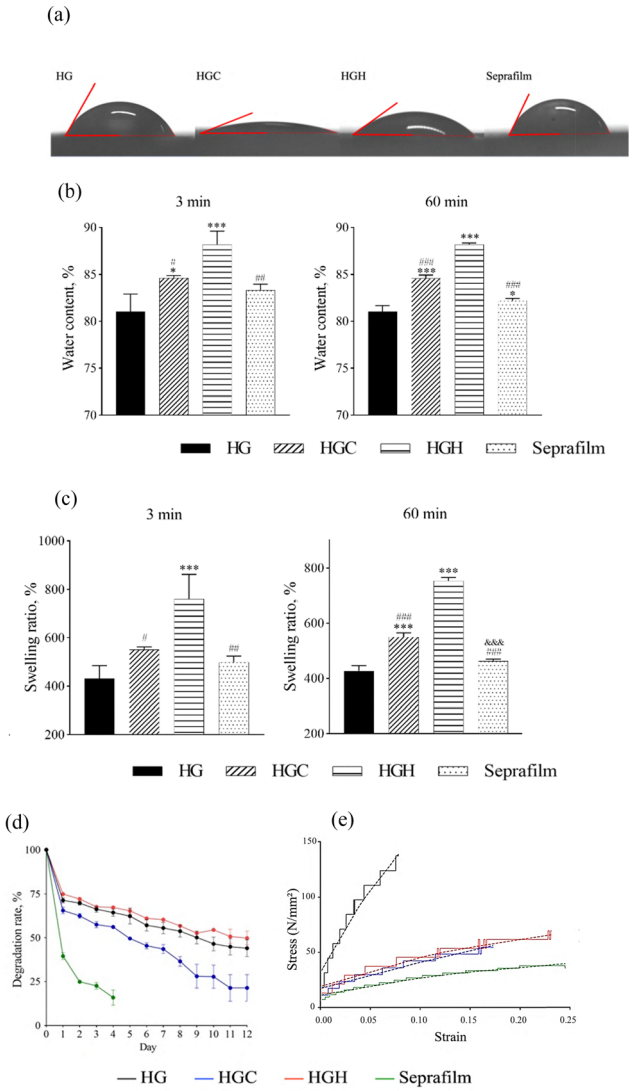

Fig. 3 Properties of hydrogel membranes: (a) images of contact angle measurements, (b) WC, (c) SR, (d) degradation rate, and (e) mechanical strength. $^{*}p < 0.05$, $^{***}p < 0.001$ compared with the control group. $^{\#}p < 0.05$, $^{\#\#}p < 0.01$, $^{\#\#\#}p < 0.001$ compared with HGH membrane ($N = 3$).

Table 2 Contact angle and tensile strength and strain of hydrogel membranes

Group ($n = 3$)	Contact angle (deg)	Tensile strength (MPa)	Strain
HG	50.6 ± 6.7	122.73 ± 19.28***	0.083 ± 0.014**
HGC	15.1 ± 0.4***	53.19 ± 9.75^{ns}	0.177 ± 0.059^{ns}
HGH	34.9 ± 7.6**	69.44 ± 12.73**	0.213 ± 0.07^{ns}
Seprafilm	53.4 ± 2.5^{ns}	34.96 ± 1.59	0.226 ± 0.008

$^{**}p < 0.01$, $^{***}p < 0.001$ compared with the Seprafilmm. ns: non-significant difference.

preliminary result of improved longevity relative to Seprafilm. Longer term degradation studies (beyond 12 days) will be needed to confirm the performance over 6 weeks fully in the future.

Fig. 3e illustrates the results of the stress–strain mechanical tests for the fabricated membranes and Seprafilm. The HG membrane was found to be brittle and fragile and to exhibit the most considerable stress and lowest strain. The HGC and HGH membranes exhibited similar mechanical stress and strain properties; they became more resilient and elastic with higher strain and moderate tensile strength (stress). The Seprafilm membrane exhibited the lowest stress, possibly because of its high HA content (nearly 66 wt%). Notably, the HGH membrane exhibited moderate mechanical strength and favorably resisted deformation (high strain). Table 2 presents the contact angle, tensile strength, and strain of the membranes. In summary, the addition of HPMC during hydrogel membrane fabrication yielded a membrane that exhibited improved hydrophilicity, achieved rapid hydration equilibrium, and demonstrated higher resilience, as well as better tensile strength and strain, compared to the HG, HGC, and Seprafilm membranes. In particular, the HGH membrane degraded more slowly than the commercial Seprafilm membrane did; this characteristic is beneficial in antiadhesive barriers for slow-healing repair sites. These results suggest that the HGC and HGH membranes may address the limitations of the commercial Seprafilm membrane, meet surgical requirements, and provide an excellent antiadhesive function.

3.3 Cell viability analysis

The MTT assay results (Fig. S2) indicated that cells cultured on the HG, HGC, and HGH membranes exhibited comparable cell viability levels to those of cells grown on standard culture plates (control group). The membranes were thus nontoxic. Additionally, cells were found to be strongly attached to the membrane particles; elongated pseudopods were observed, and the cells retained their normal fibril-like shape, indicating that the cultured cells had not been harmed by inoculation with extracts from the developed membranes.

3.4 *In vivo* animal study of membranes

Sprague-Dawley rats were selected as the experimental animals for the *in vivo* study. Fig. 4a depicts the surgical procedures in which the HGC, HGH, and Seprafilm membranes were wrapped around the ruptured tendons. The HG membrane was found to attach favorably to the tendon, which maybe contributed by the benefit of its higher water swelling ratio; however, some gaps were noted between the tendons and the HGC and Seprafilm membranes (yellow arrows in Fig. 4a). Compared with the HGH membrane, the HGC and Seprafilm membranes were less plastic, more fragile, and not easily fit onto the repaired tendons during the surgical procedures. The HGH membrane was more resilient and could be fit onto the repaired tendon smoothly, indicating that this membrane was much easier to manipulate.

3.5 Macroscopic observations of peritendinous adhesion

In our study, the Ishiyama score was used to evaluate macroscopic observation of peritendon adhesions. However, the Tang grading system[30] designed for flexor tendon studies has been widely used. However, the Ishiyama 5-grade scoring system addresses a semi-quantitative criterion based on both the ease

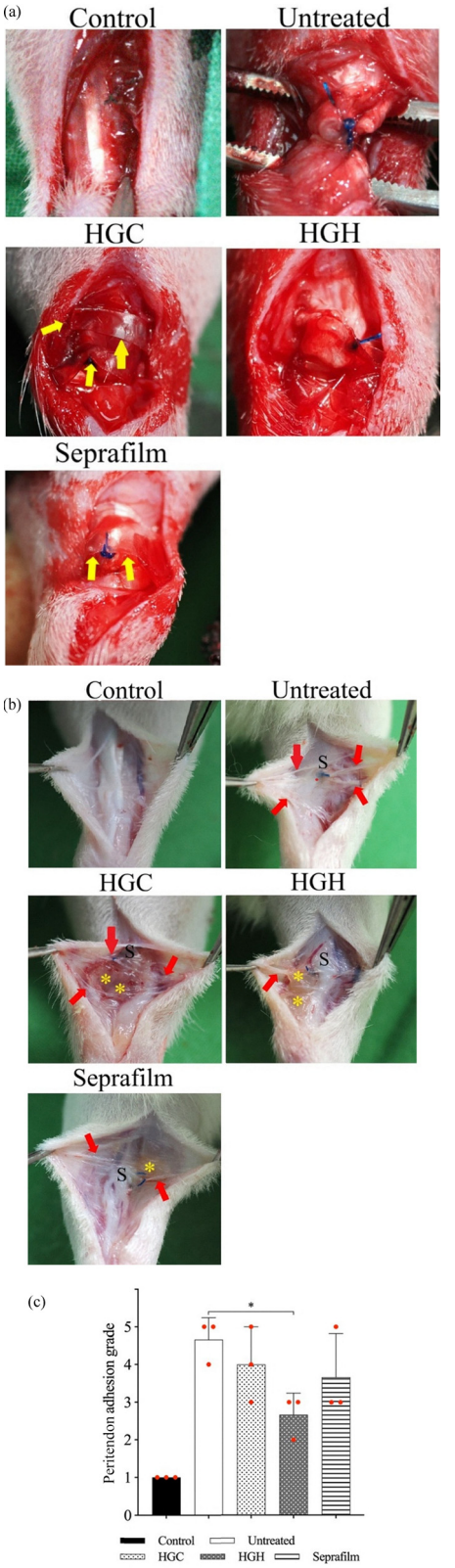

Fig. 4 (a) Macroscopic-view photographs of the control tendon, untreated repaired tendon, and repaired Achilles tendons wrapped with the HGC, HGH, or Seprafilm membrane. Yellow arrows indicate a gap between the membrane and the repaired tendon. The HGH membrane attached firmly to the tendon, with no gaps found. (b) Adhesion evaluation after 3 weeks of healing. Red arrows indicate adhesive bands. S: suture site, yellow *: residual membrane. (c) Peritendon adhesion grade of all groups. *$P < 0.05$.

of separation (blunt *vs.* sharp dissection) and the percentage of the tendon surface involved. Adhesions are classified as grade 3 if $\leq$50% requires sharp dissection, grade 4 if 51–97.5% is involved, and grade 5 if >97.5% requires sharp dissection, whereas the Tang method rely more on subjective descriptors. This method provides clear, reproducible cut-offs and greater sensitivity in distinguishing moderate from near-total adhesions. The Ishiyama method has also been adapted in many studies for the evaluation of tendon adhesion.[31–34]

Fig. 4b depicts representative macroscopic-view images of the repaired rat Achilles tendons after 3 weeks of healing. For the untreated group, adhesion was severe, as indicated by the existence of massive, dense adhesive bundles between the tendon and surrounding tissues. For the HGC and Seprafilm membrane groups, we observed fewer adhesion bundles that loosely linked the tendons and surrounding tissues. The least adhesion was observed for the HGH membrane group, and the adhesion site could be separated easily through blunt dissection. The macroscopic adhesion grades for all membrane groups were lower than the grades for the untreated group. The average grade for the HGH membrane group was significantly lower than that for the untreated group (p = 0.0321). Still, the differences between the untreated group and the HGC and Seprafilm groups were nonsignificant (p = 0.6843 and 0.3731, respectively). Residual material of the membrane was also observed in the membrane-treated groups. However more residual material in HGC and HGH groups than Seprafilm group could be observed. This *in vivo* finding was consistent with the result of *in vitro* degradation test in our study, which presented a lower degradation rate in HGH and HGC than Seprafilm.

3.6 *In vivo* histological assessments

Two hind legs in each group were used for the histological assessments of tendon adhesion and healing (Fig. 5). At the repair sites of the untreated tendons, massive fibrous tissues were found between each tendon and its surrounding tissues. Similar fibrous adhesion scars were also observed between the dermis and the tendons wrapped with the HGC or Seprafilm membrane. By contrast, the repair sites wrapped with the HGH membrane exhibited a loose subcutaneous layer with few fibrous tissues and a clear gap between the tendon and dermis. The histological observations in the HGH membrane group were similar to those in the control group, indicating that little adhesion occurred during the healing of the tendon (Fig. 5a). A grading system was employed to evaluate tendon adhesion and healing on the basis of the histological observations. As displayed in Fig. 6a, the transected tendon wrapped with the HGH membrane had a lower adhesion grade than did those in the other experimental groups, indicating that adhesion was prevented to a greater extent. Masson's trichrome staining conducted to assess tendon healing (Fig. 5b) revealed that the repaired tendon wrapped with the HGH membrane exhibited favorable continuity, as indicated by well-aligned intratendinous collagen bundles (within the yellow frame in Fig. 5b), and a smooth epitenon continuity (red arrow in Fig. 5b).

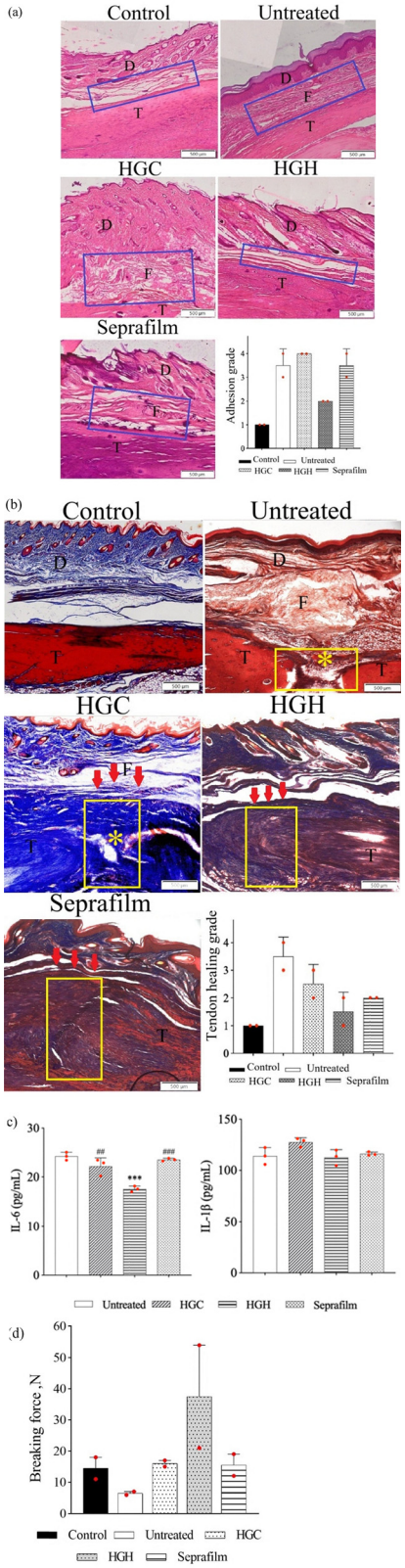

Fig. 5 (a) H&E staining and adhesion grade of repaired tendons (n = 2). Blue frame: space between dermis and tendon. T: tendon. D: dermis. F: fibrous tissue. (b) Masson's trichrome staining and healing grade of repaired tendons (n = 2). Yellow frame: anastomosis of repaired tendon. T: tendon. D: dermis. F: fibrous tissue. Yellow *: gap of anastomosis. Red arrow: epitendon. (c) Levels of inflammatory cytokines IL-6 and IL-1β in the rat tendon, assayed using ELISA. $^{*}p < 0.05$, $^{***}p < 0.001$ compared with the control group. $^{\#\#}p < 0.01$, $^{\#\#\#}p < 0.001$ compared with untreated group (N = 3) (d) Breaking force of tendons collected 3 weeks after surgery (N = 2).

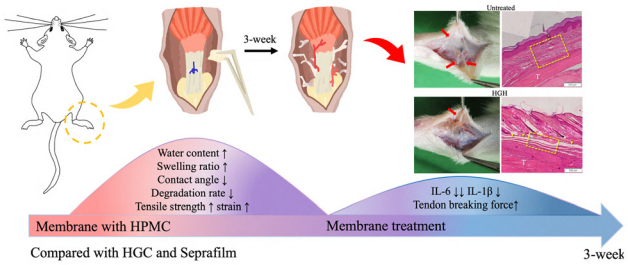

Fig. 6 Schematic of the antiadhesive HGH membrane and effects of its HPMC component (comparing with the HGC and Seprafilm membranes).

Although the tendon wrapped with the Seprafilm membrane also exhibited a favorable state of repair, with continuous intratendinous collagen bundles, less clear and loose space between the tendon and dermis than HGH group were noted. Compared with those wrapped with the HGH or Seprafilm membrane, the tendons wrapped with the HGC membrane exhibited interrupted tendon repair with partly broken intratendinous collagen bundles and irregular peritendon continuity. The bundle of fibrous tissues within the space between the dermis and tendon was also observed, indicating that adhesion had occurred. In the untreated group, a broken tendon with a gap and a large fibrous tissue between the dermis and the repaired tendon were observed, indicating inferior and incomplete repair of the ruptured tendon. Integrated and healthy tendons were found in the control group. The tendon healing grades for the HGH and Seprafilm membrane groups (approximately half of that for the untreated group) were lower than those for the HGC membrane and untreated groups, demonstrating superior healing of the tendons. Overall, the macroscopic and histological results indicate that the HGH membrane effectively prevented the repaired tendon from being invaded by surrounding fibrous tissues and did not negatively influence the healing of the injured tendon.

After 3 weeks of healing, the tissues surrounding each tendon were collected, and their inflammation was assayed through ELISA. IL-6 is a key proinflammatory cytokine that is rapidly induced during inflammation and is involved in both local and systemic inflammatory responses. As illustrated in Fig. 5c, IL-6 levels were significantly lower in the HGH membrane group (17.6 ± 0.6 pg mL^{-1}) than in the untreated group (24.2 ± 0.8 pg mL^{-1}). IL-6 levels were also significantly lower in the HGH membrane group than in the HGC and Seprafilm membrane groups (22.2 ± 1.7 pg mL^{-1}, $p < 0.01$; 23.5 ± 0.3 pg mL^{-1}, $p < 0.001$, respectively). IL-1β is a potent proinflammatory cytokine that is crucial for host defense responses to infection and injury. It plays a vital role in the defense against short-term inflammation.[35,36] As indicated in Fig. 5c, IL-1β levels were slightly lower in the HGH membrane

group (112.7 ± 7.6 pg mL^{-1}) than in the untreated group (114.1 ± 8.3 pg mL^{-1}). However, no significant differences in IL-1β levels were determined between the HGC and Seprafilm membrane groups (127.6 ± 4.4 and 116.5 ± 1.7 pg mL^{-1}, $p > 0.05$, respectively).

3.7 Breaking force measurement

The breaking force measurement results confirmed the histological healing of the tendons. Fig. 5d shows the breaking forces of the tendons; the average loads in the control, untreated, HGH membrane, HGC membrane, and Seprafilm membrane groups were 14.5, 6.5, 16, 37.5, and 15.5 N, respectively. The tendon breaking force in the Seprafilm membrane group indicated that the Seprafilm membrane had limited capacity to improve the repair of the tendon, although it prevented the adhesion of the tendon to surrounding tissues (Fig. 4c and 5a). All membrane-treated tendons achieved substantially higher breaking forces (16–37.5 N) than the untreated group (6.5 N), and notably, the HGH membrane group exhibited the highest average strength (37.5 N), surpassing not only the untreated but also the uninjured control (14.5 N). Tthe work-to-failure (energy absorption) was also measured. The HGH membrane group showed a work value of 5.89 mJ, which was markedly higher than that of the untreated (0.72 mJ), HGC (0.77 mJ), and Seprafilm (0.79 mJ) groups, and even higher than the uninjured control (3.35 mJ). The work value of control group (without any injury) was 3.35 mJ. This suggested that HGH-treated tendons not only regained tensile strength but also exhibited superior toughness and energy absorption capacity, allowing the tendon to resist rupture under greater mechanical demand. Such energy-related measures are important since they reflect the resistance to catastrophic failure and functional resilience of the repaired tendon tissue. The work value of control group (without any injury) was 3.35 mJ. As noted, the stiffness of repaired tendon wrapped with experimental membranes demonstrated much higher levels as compared to control group and untreated group, which probably caused by the healing or adhesive surrounding tissues (Table S1). Overall, the results indicate a superior healing potential of injured tendon wrapped with HGH membrane. Notably, the HGH membrane group not only presented less tendon adhesion and better tendon healing in histology (Fig. 5a and b) but also had a significantly higher breaking force than the HGC and Seprafilm membrane groups did, indicating superior healing of the tendons. The biomechanical results align with the histological and gross findings: the HGH membrane promoted superior tendon healing. This could be explained by the fact that reduced adhesions allow the tendon glide better and the collagen align well to promote healing and improved the mechanical strength of tendon. This is consistent with previous animal tendon healing studies, which emphasized the correlation with biomechanical properties and tendon repair strength. For example, Hammerman *et al.* reported that peak force reliably reflects the quality of healing in rat Achilles tendon repair.[37] Likewise, Ghayemi *et al.* demonstrated in a rabbit tendon model that therapeutic interventions improved not only ultimate load but also stiffness and energy absorption, emphasizing the value of complementary parameters.[38]

Tendon adhesions were previously believed to be a natural part of the tendon healing process. Progressive peritendinous adhesions bind a healing or healed tendon to surrounding tissues, leading to a delay in tendon healing or to functional disability, which may eventually result in decreased strength and ability.[39] The administration of a barrier membrane is among the most common strategies for preventing postsurgical adhesion. Several studies have used films or hydrogel membrane complexes containing hyaluronic acid, chitosan, and alginate as physical barriers to prevent adhesion.[39,40] Seprafilm and ADEPT are two commonly used antiadhesion barrier products approved and regulated by the FDA.[41] Seprafilm is usually placed directly on a flat site to prevent adhesion to surrounding tissues. CMC, a component of Seprafilm, is widely used in the pharmaceutical and food industries as a viscosity modifier, emulsifier, and stabilizer for dosage formulations. Although CMC has excellent water swelling ability, nontoxicity, and biodegradability, it degrades rapidly in bodily fluids owing to its hydrophilicity and weak enzyme resistance. Additionally, the poor strength and fragility of CMC engender difficulties in manipulating it during surgery or placing it onto nonflat tendon tissue. Many researchers have blended bioactive compounds into membrane materials to prepare antiadhesive membranes with anti-inflammatory properties, enhanced tissue repair capabilities, or additional therapeutic functions beyond adhesion prevention.[42,43] Lin *et al.* prepared CMC bilayer-structure membranes incorporating *Bletilla striata* polysaccharide to prevent postoperative adhesion, reduce inflammation, and improve tendon repair.[44,45] Although this bilayer demonstrated promising results and provided a potential alternative for tendon repair, the added polysaccharide could have diverse and unpredictable effects, which could pose challenges for commercialization.

HPMC was selected as an alternative antiadhesion material in this study mainly because it is highly soluble owing to its numerous hydrophilic hydroxyl groups. The addition of HPMC to a liquid system increases the system's viscosity because of high intermolecular friction among solvated HPMC chains.[46] HPMC is frequently utilized as a thickener and stabilizer in food and drug formulations. Therefore, researchers are seeking formulations that offer the best possible pharmacotherapy, such as combinations of HPMC with other polymers or additives to tune and control a material's characteristics or imbue the material with noninherent characteristics.[47]

The low cost and rapid gelation of FDA-approved GA could make it extremely useful in a clinical setting. GA can remain at a repair site for several weeks, which is advantageous when considering the tendon healing timeframe. HA is recognized as an essential compound for preventing peritendinous adhesion. However, unlike HPMC and GA, HA is rapidly degraded by hyaluronidase and disappears from a repair site within days. A barrier membrane should remain in place long enough to support healing at the target repair site and should be easy to manipulate during surgical procedures. Moreover, such a

membrane should degrade slowly, have moderate strength, be resilient, and rapidly reach hydration equilibrium, in addition to preventing fibrous tissue ingrowth, which impedes the healing of tendons. In summary, our findings indicate the following benefits of HPMC:

1. It delays degradation of an antiadhesion membrane (as shown in the HGH membrane group).

2. A membrane containing HPMC (the HGH membrane) rapidly equilibrates in aqueous solution and is thus easily applied during surgery.

3. A membrane containing HPMC is resilient and exhibits better strength and strain than other membranes do; it can thus be applied at more complex surgical sites.

To demonstrate the benefits of the HGH membrane, this study compared it with the commercial Seprafilm product. The benefits of the HGH membrane may be attributed to the addition of HPMC to the fabrication mixture; HPMC results in the interactions of GA and HA molecules with hydrophilic and hydrophobic groups in the polymer matrix, and these interactions delay degradation. Regardless of the architecture of the HPMC matrix, when it comes into contact with biological fluid or water, water molecules wet the HPMC chains in the uppermost (outermost) layer, and the HPMC chains become hydrated. Water molecule diffusion is more extensive when HPMC is present, and the HGH membrane thus reaches hydration equilibrium rapidly. However, this study observed that the HGC membrane exhibited much lower WC and degraded more rapidly owing to its numerous hydrophilic hydroxyl groups, although it did exhibit comparable mechanical properties to those of the HGH membrane (Fig. 3 and Table 2). Furthermore, FTIR analysis confirmed that GA, HA, and HPMC had been successfully integrated into a crosslinked hydrogel network (GA–CONH–HA/HPMC) through both physical (hydrogen bonding) and chemical (amide and ester) interactions; these probably contributed to the slow degradation of the HGH membrane (Fig. 2c).

Recent studies have suggested that the inflammatory cytokines IL-6 and IL-1β are involved in tendon repair and inflammatory responses that affect postsurgical adhesion and healing.[48] IL-6 has both proinflammatory and anti-inflammatory effects; it is essential for the initial inflammatory response and subsequent healing, but prolonged or excessive IL-6 signaling can facilitate the migration of reparative fibroblasts from the extrinsic compartment (epitenon and paratenon) to the damaged core of the tendon and is detrimental to tendon health. Excessive or prolonged IL-6 signaling may contribute to chronic tendinopathy and impede healing. However, IL-6 plays a complex (sometimes contradictory) role in tendon repair, and its effects depend on the local inflammatory environment and specific phase of repair.[49] In this study, IL-6 levels were significantly lower in the HGH membrane group than in the untreated group and were significantly lower in the HGH membrane group than in the HGC and Seprafilm membrane groups; these findings indicate that the inflammatory response was rapid and less intense after 3 weeks of healing (Fig. 5c). IL-1β, a proinflammatory cytokine, plays a complex role in tendon repair. Some studies have suggested that IL-1β can benefit tendon repair by enhancing the immunoregulatory and paracrine capabilities of mesenchymal stem cells.[50] The timing of IL-1β modulation is critical to tendon repair. In contrast to IL-6 expression, IL-1β expression did not clearly differ between the experimental groups, although it was slightly lower in the HGH group (Fig. 5c). The lower IL-6 and IL-1β levels under HGH membrane treatment resulted in superior healing of tendon, as evidenced by significantly higher breaking force (Fig. 5d). However, further investigation is warranted to explore the complex interplay of IL-6 and the optimal timing and strategies for modulating IL-1β activity to promote tendon healing.

The complications of postoperative adhesion between the tendon and surrounding tissue will delay repairs of the tendon. Nowadays, barrier is one common way to prevent postoperative adhesion used hyaluronic acid, alginate or synthetic polymers CMC, in the form of hydrogels, films, or fibers to reduce the adhesion of tendon. Lin *et al.* developed bilayer structure CMC membrane containing Bletilla striata extract for the antiadhesion and tendon repair.[44] *In vivo* animal experiment results show that effectively reduced postoperative tendon-peripheral tissue adhesion and improved tendon repair with downregulating inflammatory cytokines and increased tendon strength. Liang *et al.* developed asymmetric hydrogel using poly(acrylic acid), gelatin, and hyperbranched polymers to surgical application.[51] They demonstrated that this hydrogel could completely seal the surgical and promote the healing process, with reduced risk of postoperative tissue adhesion. The above two researchers showed that the materials used could regulates the inflammatory responses at the surgical site to reduce the occurrence of adhesion and enhance the healing. To ensure the safety of the materials used and ease of commercialization, only FDA-approved materials were employed in the fabrication of hydrogel membrane. The merits of used HPMC, GG and HA materials in fabricated hydrogel membranes were fully utilized and evaluated in tendon repair in this present study.

Fig. 6 presents a schematic of the effects of the HPMC component of the fabricated membrane in this study. The data indicated that the HPMC component resulted in increased WC, SR, and mechanical strength and strain. It also led to less rapid degradation than that observed for the HGC and Seprafilm membranes. As confirmed by the results of our gross observation, H&E staining, Masson's trichrome staining, inflammation analyses, and breaking force measurements in the animal study, the HGH membrane led to superior tendon healing, with reduced peritendinous adhesion, alleviated inflammatory responses, and increased breaking force. However, these results should be considered preliminary. This is because we used a rat model to simulate postoperative adhesion of the Achilles tendon, but larger animals or humans may require a longer physiological healing period (typically 4–6 weeks). Additionally, in accordance with the 3Rs (reduction, replacement, refinement) principle of animal research, only two or three Achilles tendon samples per group were used for analysis. Accordingly, the limitations of this study include its small animal sample and short follow-up time. A larger sample and longer follow-up may be required to study tendon healing in the

future to ensure the HGH membrane can be applied in Achilles tendon repair.

4. Conclusions

In summary, the HGH membrane, which contains HPMC, more rapidly reached equilibrium; had higher hydrophilicity, lower WC, and higher mechanical strength and strain; and was easier to manage during surgery than the other investigated membranes. The HGH membrane degraded slowly, exhibited better antiadhesion ability, and had significantly higher breaking force compared with the HGC and Seprafilm membranes; these results thus demonstrate its potential value as an alternative to the commercial Seprafilm product in prevention of peritendon adhesion as tendon repair applications. In particular, all materials used to develop the antiadhesion HGH membranes are FDA approved. The use of these materials could expedite or simplify the regulatory process for commercializing the product, particularly regarding concerns about material safety and origin.

Author contributions

Shan-Wei Yang – methodology, conceptualization, funding acquisition. Mu-Ting Li – formal analysis, validation, data curation. Chun-Shien Wu – validation, formal analysis. Joseph Yang – validation. Daniel Yang – validation. Shyh-Ming Kuo – writing – editing & review, validation, project administration, methodology, funding acquisition, conceptualization.

Conflicts of interest

The authors declare no conflict of interests.

Data availability

Data will be available on request.

Supplementary information is available. See DOI: **https://doi.org/10.1039/d5tb01703c**.

Acknowledgements

This study was funded by the grants from Ministry of Science and Technology, Taiwan (NSTC 113-2314-B-214-005-MY2).

References

1 T. K. Rajab, M. Wallwiener and S. Talukdar, *et al.*, Therapeutic strategies for the prevention of postoperative adhesions in gynaecological surgery – a systematic review, *Hum. Reprod. Update*, 2010, **16**, 319–329.
2 W. W. Vrijland, J. Jeekel, H. J. Van Geldorp, D. J. Swank and H. J. Bonjer, Abdominal adhesions: intestinal obstruction, pain, and infertility, *Surg. Endoscopy Interventional Tech.*, 2003, **17**(7), 1.
3 R. P. Ten Broek, C. Strik, Y. Issa, R. P. Bleichrodt and H. van Goor, Adhesiolysis-related morbidity in abdominal surgery, *Ann. Surg.*, 2013, **258**(1), 98–106.
4 M. P. Diamond and M. L. Freeman, Clinical implications of postsurgical adhesions, *Hum. Reprod. Update*, 2001, **7**(6), 567–576.
5 Y. Wu, L. Wang, B. Guo and P. X. Ma, Injectable Biodegradable Hydrogels and Microgels Based on Gallic Acid–PEG Conjugates for Tissue Engineering, *Biomaterials*, 2021, **276**, 121024.
6 Z. Tang, R. Zhang, X. Zhang, Y. Xu, M. Wang and Q. Shen, *et al.*, Tannic acid inspired self-crosslinking hydrogel for preventing postoperative adhesion, *ACS Appl. Mater. Interfaces*, 2020, **12**(24), 26869–26877.
7 X. Li, Y. Dai, T. Shen, Y. Xue and X. Zhang, A dopamine-based hydrogel for preventing post-surgical adhesion, *Mater. Sci. Eng., C*, 2020, **117**, 111273.
8 J. H. Ryu, P. B. Messersmith and H. Lee, Polydopamine surface chemistry: a decade of discovery, *ACS Appl. Mater. Interfaces*, 2018, **10**(9), 7523–7540.
9 Baxter Inc., What is Seprafilm? (Seprafilm product information page), accessed 2023: **https://advancedsurgery.baxter.com/what-is-Seprafilm**.
10 C. S. Hsu and D. C. Ding, Feasibility of wet and non-wet placement of Seprafilm in laparoscopic surgeries: a randomized controlled trial, *J. Clin. Med.*, 2021, **10**(16), 3526.
11 M. P. Diamond, E. L. Burns, B. Accomando, S. Mian and L. Holmdahl, Seprafilm® adhesion barrier:(2) a review of the clinical literature on intraabdominal use, *Gynecolog. Surgery*, 2012, **9**(3), 247–257.
12 Baxter Inc., Adhesion Prevention in Gynecology (Seprafilm precautions), accessed 2023, **https://advancedsurgery.baxter.com/adhesion-prevention-gynecology**.
13 Q. Zeng, Z. Yu, J. You and Q. Zhang, Efficacy and safety of Seprafilm for preventing postoperative abdominal adhesion: systematic review and meta-analysis, *World J. Surg.*, 2007, **31**(11), 2125–2131.
14 R. Ghadermazi, S. Hamdipour, K. Sadeghi, R. Ghadermazi and A. Khosrowshahi Asl, Effect of various additives on the properties of the films and coatings derived from hydroxypropyl methylcellulose—A review, *Food Sci. Nutrition*, 2019, **7**(11), 3363–3377.
15 D. E. Beck, Z. Cohen, J. W. Fleshman, H. S. Kaufman, H. van Goor and B. G. Wolff, A prospective, randomized, multicenter, controlled study of the safety of Seprafilm® adhesion barrier in abdominopelvic surgery of the intestine, *Dis. Colon Rectum*, 2003, **46**(10), 1310–1319.
16 J. Siepmann and N. A. Peppas, Modeling of drug release from delivery systems based on hydroxypropyl methylcellulose (HPMC), *Adv. Drug Delivery Rev.*, 2012, **64**, 163–174.
17 C. Jin, F. Wu, Y. Hong, L. Shen, X. Lin, L. Zhao and Y. Feng, Updates on applications of low-viscosity grade Hydroxypropyl methylcellulose in coprocessing for improvement of physical properties of pharmaceutical powders, *Carbohydr. Polym.*, 2023, **311**, 120731.
18 L. L. Tundisi, G. B. Mostaço, P. C. Carricondo and D. F. S. Petri, Hydroxypropyl methylcellulose: physicochemical

properties and ocular drug delivery formulations, *Eur. J. Pharm. Sci.*, 2021, **159**, 105736.
19 S. Habibullah, J. R. Meher, M. Das, T. Das, R. Swain, B. Mohanty and S. Mallick, Moxifloxacin in HPMC-nanocellulose composite film for the management of ocular inflammation: effect of carboxymethylated gum on permeation and antimicrobial activity, *Int. J. Biol. Macromol.*, 2025, 143302.
20 K. Dharmalingam and R. Anandalakshmi, Fabrication, characterization and drug loading efficiency of citric acid crosslinked NaCMC-HPMC hydrogel films for wound healing drug delivery applications, *Int. J. Biol. Macromol.*, 2019, **134**, 815–829.
21 M. S. Rahman, M. S. Hasan, A. S. Nitai, S. Nam, A. K. Karmakar, M. S. Ahsan and M. B. Ahmed, Recent developments of carboxymethyl cellulose, *Polymers*, 2021, **13**(8), 1345.
22 F. S. Palumbo, S. Federico, G. Pitarresi, C. Fiorica and G. Giammona, Gellan gum-based delivery systems of therapeutic agents and cells, *Carbohydr. Polym.*, 2020, **229**, 115430.
23 D. Gomes, J. P. Batista-Silva, A. Sousa and L. A. Passarinha, Progress and opportunities in Gellan gum-based materials: a review of preparation, characterization and emerging applications, *Carbohydr. Polym.*, 2023, **311**, 120782.
24 R. A. K. Abdl Aali and S. T. G. Al-Sahlany, Gellan gum as a unique microbial polysaccharide: its characteristics, synthesis, and current application trends, *Gels*, 2024, **10**(3), 183.
25 D. Kim, H. H. Cho, M. Thangavelu, C. Song, H. S. Kim, M. J. Choi and G. Khang, Osteochondral and bone tissue engineering scaffold prepared from Gallus var domesticus derived demineralized bone powder combined with gellan gum for medical application, *Int. J. Biol. Macromol.*, 2020, **149**, 381–394.
26 Y. Chen, Y. Liu, J. Xie, Q. Zheng, P. Yue, L. Chen and M. Yang, Nose-to-brain delivery by nanosuspensions-based in situ gel for breviscapine, *Int. J. Nanomed.*, 2020, 10435–10451.
27 N. Ishiyama, T. Moro, K. Ishihara, T. Ohe, T. Miura, T. Konno and H. Kawaguchi, The prevention of peritendinous adhesions by a phospholipid polymer hydrogel formed in situ by spontaneous intermolecular interactions, *Biomaterials*, 2010, **31**(14), 4009–4016.
28 S. Liu, C. Hu, F. Li, X. J. Li, W. Cui and C. Fan, Prevention of peritendinous adhesions with electrospun lbuprofen-loaded poly(L-lactic acid)-polyethylene glycol fibrous membranes, *Tissue Eng., Part A*, 2013, **19**(3–4), 529–537.
29 N. Xia, Y. Xing, G. Wang, Q. Feng, Q. Chen, H. Feng and L. Liu, Probing of EDC/NHSS-mediated covalent coupling reaction by the immobilization of electrochemically active biomolecules, *Int. J. Electrochem. Sci.*, 2013, **8**(2), 2459–2467.
30 J. B. Tang, S. Ishii, U. Masamichi and M. Aoki, Dorsal and circumferential sheath reconstructions for flexor sheath defect with concomitant bony injury, *J. Hand Surgery*, 1994, **19**(1), 61–69.
31 H. Ruan, S. Liu, F. Li, X. Li and C. Fan, Prevention of tendon adhesions by ERK2 small interfering RNAs, *Int. J. Mol. Sci.*, 2013, **14**(2), 4361–4371.
32 W. Zheng, J. Song, Y. Zhang, S. Chen, H. Ruan and C. Fan, Metformin prevents peritendinous fibrosis by inhibiting transforming growth factor-β signaling, *Oncotarget*, 2017, **8**(60), 101784.
33 C. H. Hsu, P. Chen, C. P. Yang, C. A. Chuang, Y. S. Chan and J. C. H. Chiu, The results of preventing postoperative achilles tendon adhesion using cross-linked and non-cross-linked hyaluronic acid, a study with rat model, *J. Orthop. Surg. Res.*, 2024, **19**(1), 457.
34 J. Yang, J. He and L. Yang, Advanced glycation end products impair the repair of injured tendon: a study in rats, *BMC Musculoskeletal Disord.*, 2024, **25**(1), 700.
35 J. S. Ainscough, G. F. Gerberick, M. Zahedi-Nejad, G. Lopez-Castejon, D. Brough, I. Kimber and R. J. Dearman, Dendritic cell IL-1α and IL-1β are polyubiquitinated and degraded by the proteasome, *J. Biol. Chem.*, 2014, **289**(51), 35582–35592.
36 J. Khan, N. Noboru, A. Young and D. Thomas, Pro and anti-inflammatory cytokine levels (TNF-α, IL-1β, IL-6 and IL-10) in rat model of neuroma, *Pathophysiology*, 2017, **24**(3), 155–159.
37 M. Hammerman, F. Dietrich-Zagonel, P. Blomgran, P. Eliasson and P. Aspenberg, Different mechanisms activated by mild versus strong loading in rat Achilles tendon healing, *PLoS One*, 2018, **13**(7), e0201211.
38 N. Ghayemi, F. Sarrafzadeh-Rezaei, H. Malekinejad, M. Behfar and A. A. Farshid, Effects of rabbit pinna-derived blastema cells on tendon healing, *Iran. J. Basic Med. Sci.*, 2020, **23**(1), 13.
39 N. Yuan, K. Shao, S. Huang and C. Chen, Chitosan, alginate, hyaluronic acid and other novel multifunctional hydrogel dressings for wound healing: a review, *Int. J. Biol. Macromol.*, 2023, **240**, 124321.
40 I. Silvestro, M. Lopreiato, A. Scotto d'Abusco, V. Di Lisio, A. Martinelli, A. Piozzi and I. Francolini, Hyaluronic acid reduces bacterial fouling and promotes fibroblasts' adhesion onto chitosan 2D-wound dressings, *Int. J. Mol. Sci.*, 2020, **21**(6), 2070.
41 R. J. Morris III, T. Nori, A. D. Sandler and P. Kofinas, Post-operative Adhesions: Current Research on Mechanisms, Therapeutics and Preventative Measures, *Biomed. Mater. Devices*, 2024, 1–41.
42 M. S. Rahman, M. S. Hasan, A. S. Nitai, S. Nam, A. K. Karmakar, M. S. Ahsan and M. B. Ahmed, Recent developments of carboxymethyl cellulose, *Polymers*, 2021, **13**(8), 1345.
43 I. M. Flutur, D. N. Păduraru, A. Bolocan, A. C. Palcău, D. Ion and O. Andronic, Postsurgical adhesions: is there any prophylactic strategy really working?, *J. Clin. Med.*, 2023, **12**(12), 3931.
44 Z. Y. Chen, S. H. Chen, S. H. Chen, P. Y. Chou, C. Y. Kuan, I. H. Yang and F. H. Lin, Bletilla striata polysaccharide-containing carboxymethyl cellulose bilayer structure membrane for prevention of postoperative adhesion and achilles tendon repair, *Biomacromolecules*, 2024, **25**(9), 5786–5797.
45 Z. Y. Chen, S. H. Chen, S. H. Chen, P. Y. Chou, C. Y. Kuan, I. H. Yang and F. H. Lin, Bletilla striata polysaccharide-containing carboxymethyl cellulose bilayer structure membrane for prevention of postoperative adhesion and achilles tendon repair, *Biomacromolecules*, 2024, **25**(9), 5786–5797.
46 C. Jin, F. Wu, Y. Hong, L. Shen, X. Lin, L. Zhao and Y. Feng, Updates on applications of low-viscosity grade Hydroxypropyl

methylcellulose in coprocessing for improvement of physical properties of pharmaceutical powders, *Carbohydr. Polym.*, 2023, **311**, 120731.

47 L. L. Tundisi, G. B. Mostaço, P. C. Carricondo and D. F. S. Petri, Hydroxypropyl methylcellulose: physicochemical properties and ocular drug delivery formulations, *Eur. J. Pharm. Sci.*, 2021, **159**, 105736.

48 F. Jiang, H. Zhao, P. Zhang, Y. Bi, H. Zhang, S. Sun and X. Xiao, Challenges in tendon–bone healing: emphasizing inflammatory modulation mechanisms and treatment, *Front. Endocrinol.*, 2024, **15**, 1485876.

49 E. Chisari, L. Rehak, W. S. Khan and N. Maffulli, Tendon healing is adversely affected by low-grade inflammation, *J. Orthop. Surg. Res.*, 2021, **16**(1), 700.

50 S. Wang, Z. Yao, L. Chen, J. Li, S. Chen and C. Fan, Preclinical assessment of IL-1β primed human umbilical cord mesenchymal stem cells for tendon functional repair through TGF-β/IL-10 signaling, *Heliyon*, 2023, **9**(11), 1–15.

51 L. Liang, X. Li, Z. Tan, M. Liu, Y. Qiu, Q. Yu and J. Li, Injectable spontaneously formed asymmetric adhesive hydrogel with controllable removal for wound healing, *J. Mater. Chem. B*, 2023, **11**(45), 10845–10858.

